Electronic and Infrared Spectroscopy of [Benzene−(Methanol)$_n$]$^+$ (n = 1−6)

Satoko Enomoto, Mitsuhiko Miyazaki,§ Asuka Fujii,* and Naohiko Mikami*

Department of Chemistry, Graduate School of Science,Tohoku University, Sendai 980-8578, Japan

Received: April 30, 2005; In Final Form: July 27, 2005

The microsolvation structure of the [benzene−(methanol)$_n$]$^+$ (n = 1−6) clusters was analyzed by electronic and infrared spectroscopy. For the n = 1 and 2 clusters, further spectroscopic investigation was carried out by Ar atom attachment, which has been know as a useful technique for discriminating isomers of the clusters. The coexistence of multiple isomers was confirmed for the n = 1 and 2 clusters, and remarkably, preferential production of the specific isomers occurred in the Ar attachment. The most stable isomer of the n = 1 cluster was suggested to be of the "on-ring" structure where the nonbonding electrons of the methanol moiety directly interact with the π orbital of the benzene cation moiety. This is a sharp contrast to [benzene−(H$_2$O)$_1$]$^+$, exhibiting the "side" structure, where the water moiety is bound to the C−H sites of the benzene cation moiety. The structure of the n = 2 cluster was discussed with the help of density functional theory calculations. Spectral signatures of the intracluster proton-transfer reaction were found for $n \geq 5$. The intracluster electron-transfer reaction leading to the (methanol)$_m^+$ fragment was also seen upon vibrational and electronic excitation of $n \geq 4$.

I. Introduction

Gas-phase clusters of organic or inorganic molecular cations surrounded by solvent molecules have been extensively studied using various spectroscopic methods in combination with supersonic molecular beams.[1−4] Since such well-defined clusters are considered to be microscopic model systems of the solvation in bulk, they are quite useful for structural investigation of microsolvation, in which their intermolecular structures are determined by the competition among various intermolecular forces, such as electrostatic interactions, charge-induced interactions, charge-transfer interactions, hydrogen bonds, and so on. In the case of the clusters of an aromatic cation surrounded by polar solvent molecules, more dynamical effects might occur to lead intracluster chemical reactions.[3,4]

Benzene−water cluster cations, [Bz−(H$_2$O)$_n$]$^+$, are a prototype system for the microsolvation of aromatic cations with polar solvents.[4−17] Mass spectrometry and theoretical approaches have been applied to characterize this system.[3,5−10] Recently, our group and Dopfer et al. have extensively studied the cluster structures by electronic and infrared (IR) spectroscopy in combination with ab initio/density functional theory (DFT) calculations.[4,11−17] For the n = 1 cluster, the most stable isomer was found to be of the "side" structure, where the water moiety locates in the aromatic ring plane being bound by the charge−dipole interaction as well as by the CH−O hydrogen bonds. This structure was clearly confirmed by the IR spectroscopic studies and was also supported by theoretical calculations.[5,9−13,16,17] For the n = 2 cluster, on the other hand, two species were found to exist as stable isomers. The DFT calculations predicted that the most stable isomer includes a hydrogen-bonded water dimer subunit, while the IR spectral signature of two separately solvating water molecules was also suggested.[12,17] Such coexistence of these structural isomers was shown by the dependence of the IR spectra on the cluster-ion preparation methods, demonstrating that the charge−dipole interaction between the benzene cation and water molecules competes with the hydrogen bond between the water molecules.[4,12,17] With respect to this point, the microsolvation structures of the [Bz−(H$_2$O)$_n$]$^+$ cluster cations are totally different from those of the corresponding to the neutral Bz−(H$_2$O)$_n$ clusters, where the water subunit is bound on the top of the aromatic ring by the π-hydrogen bond.[18,19] Extensive rearrangement of the cluster structure upon ionization has been predicted on the basis of theoretical calculations and the experimental observation of the high fragmentation yield upon ionization.[5,9,20] Drastic structural changes following ionization were actually confirmed by the IR spectroscopy of the cluster cations prepared by the resonantly enhanced multiphoton ionization (REMPI).[11,12] On the other hand, the IR spectra of the [Bz−(H$_2$O)$_n$]$^+$ clusters with the larger size, $n \geq 4$, showed features very similar to those of H$^+$(H$_2$O)$_{n+1}$, suggesting that the intracluster proton-transfer reaction takes place to form the hydrated hydronium ion.[12,14] This size-dependent reaction was confirmed by electronic spectroscopy of the benzene moiety, as well as by the estimation of the size-dependent proton affinity of the water clusters.[15]

In contrast with the extensive studies on [Bz−(H$_2$O)$_n$]$^+$, the microsolvation of the benzene cation with methanol (MeOH) has scarcely been studied.[4,17] Methanol is a prototype molecule of alcohol, which is an important class of polar solvents in addition to water. Moreover, methanol has a larger proton affinity than water (180 and 165 kcal/mol, respectively),[21] while its dipole (1.7 D) is smaller than that of water (1.854 D).[22] Such differences in the proton affinity and dipole moment are expected to lead to a different architecture of solvation. IR spectroscopy of [Bz−(MeOH)$_n$]$^+$ has been carried out for n = 1 and 2 by Solcà and Dopfer, and to our knowledge, this has been a unique study on this system, so far.[4,17] The free OH stretch band of the methanol moiety was observed in the IR spectra of these clusters, and the clusters were estimated to have structures similar to that of [Bz−(H$_2$O)$_n$]$^+$. Details of the

* Corresponding authors. E-mail: asuka@qclhp.chem.tohoku.ac.jp (A.F.); nmikami@qclhp.chem.tohoku.ac.jp (N.M.).

§ Present address: Institute for Molecular Science, Okazaki 444-8585, Japan.

10.1021/jp052252y CCC: $30.25
Published on Web 09/30/2005

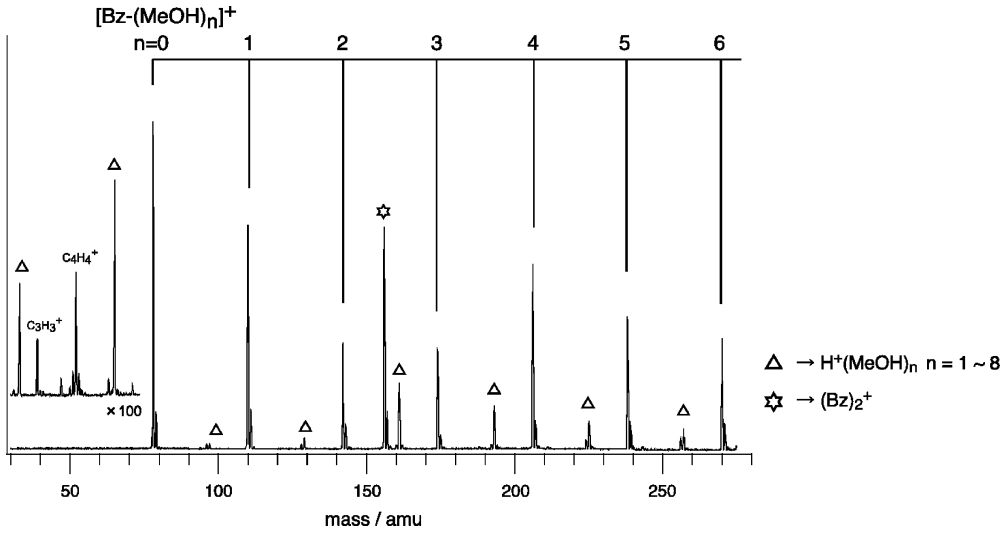

Figure 1. Mass spectrum of $[Bz-(MeOH)_n]^+$ and other ions produced in the ion source under the Ne carrier condition.

structures, however, were not analyzed because of the limited spectral information.

In this study, we present a comprehensive report on the microsolvation structure of the benzene cation with methanol. We observed IR spectra of $[Bz-(MeOH)_n]^+$ ($n = 1-6$) in the OH and CH stretching vibrational region. In addition, the electronic spectra of the $n = 1$ to 5 clusters were measured to probe solvation effects on the electronic structure of the benzene moiety. We also observed both the IR and electronic spectra of $[Bz-(MeOH)_n\text{-}Ar]^+$ ($n = 1$ and 2). The attachment of an Ar atom strictly restricts the internal energy (vibrational energy) of the cluster because of the weak binding energy to the Ar atom,[23,24] and spectra of the internally cold clusters can be observed.[4,13,24] In comparison with the spectra of the clusters with and without Ar (i.e., cold and hot clusters), we discuss the presence of structural isomers in these cluster cations. Size-dependent intracluster proton and electron-transfer reactions in the larger cluster are also examined on the basis of IR and electronic spectroscopy.

II. Experimental Section

In the experiment, we used a tandem quadrupole mass (Q-mass) filter-type spectrometer combined with a pickup-type cluster cation source.[11−15] Briefly, a gaseous mixture of benzene, methanol, and Ne (for $[Bz-(MeOH)_n]^+$) or Ar (for $[Bz-(MeOH)_n-Ar]^+$) was expanded into a source chamber through a pulsed nozzle with a stagnation pressure of 3 atm. Bare benzene molecules were resonantly ionized via the S_1-S_0 6^1_0 transition in the collisional region of the jet expansion, and the following collisions with methanol and Ne (or Ar) result in the $[Bz-(MeOH)_n]^+$ or $[Bz-(MeOH)_n-Ar]^+$ cluster formation. It has been known that such a pickup-type cluster ion source tends to produce the most stable isomer of the cluster cations because the collisional process cools the clusters.[4] The clusters produced were mass-selected by the first Q-mass filter. The mass-selected cluster cations were introduced into an octopole ion guide, where they were irradiated by a counter-propagating IR or visible-laser pulse. Because the photoabsorption results in the dissociation of the cluster cations, action spectra corresponding to the absorption spectra of the size-selected cluster cations were recorded by scanning the dissociation laser wavelength while detecting the fragment species selected by the second Q-mass filter. For electronic spectroscopy, the benzene cation fragment was mainly monitored, while the fragment cluster cation because of the evaporation of one methanol molecule or Ar atom was mainly detected in the IR spectroscopy of $[Bz-(MeOH)_n]^+$ or $[Bz-(MeOH)_n-Ar]^+$, respectively.

The pulsed-IR light for IR spectroscopy was generated by difference frequency mixing (DFM) between the fundamental outputs of a YAG laser (Spectra Physics GCR-230) and a dye laser (Lambda Physik Scanmate, LDS759+Styryl9M dyes) in a $LiNbO_3$ crystal. The visible photodissociation light for electronic spectroscopy was the output of an optical parametric oscillator (GWU, VisIR2−170) with a line width of 5−10 cm^{-1} which was pumped by a third harmonics of a YAG laser output (Continuum, Surelite III).

III. Results and Discussion

1. Cluster-Ion Production. The mass distribution of the cluster ions produced by the present ion source is seen in the mass spectrum reproduced in Figure 1. Collisional cooling of the benzene cation by methanol and buffer Ne produces the $[Bz-(MeOH)]_n^+$ cluster cation as the main products. Proton transfer from the benzene cation to methanol efficiently occurs, and a series of the protonated methanol clusters, $H^+(MeOH)_n$, is seen in the mass spectrum. It is worth noting that $(MeOH)_n^+$ cluster cations are also produced, though their intensity is weaker than that of $H^+(MeOH)_n$. The production of $(MeOH)_n^+$ upon REMPI of neutral $Bz-(MeOH)_n$ clusters has been reported by Zwier and co-workers.[25]

2. Structure of the $n = 1$ Cluster. Figure 2b and c show the electronic spectra of $[Bz-(MeOH)_1]^+$ and $[Bz-(MeOH)_1-Ar]^+$, respectively, obtained by monitoring the benzene cation fragment. The electronic spectrum of $[Bz-(H_2O)_1]^+$ is also reproduced in Figure 2a for a comparison.[15] In the visible region, the electronic transition of the benzene cation moiety is expected. In the spectrum of $[Bz-(H_2O)_1]^+$, a strong absorption appears only above 20 000 cm^{-1}. This absorption corresponds to the C−X (π, π) transition in the bare benzene cation,[26,27] which represents a minor perturbation from the water moiety to the electronic structure of the benzene cation site. The spectrum of $[Bz-(MeOH)_1]^+$ (Figure 2b) shows a similar absorption above 20 000 cm^{-1}, but an additional weak absorption is also seen in the region below 20 000 cm^{-1}. This absorption has no correspondence in the electronic spectra of the bare benzene cation nor that of $[Bz-(H_2O)_1]^+$ as shown in Figure 2a,[15] and it indicates a strong perturbation to the electronic structure of the benzene cation moiety.

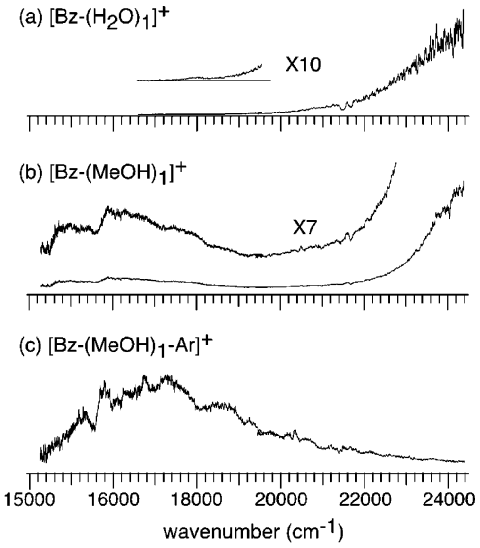

Figure 2. Electronic spectra of (a) [Bz−(H$_2$O)$_1$]$^+$, (b) [Bz−(MeOH)$_1$]$^+$, and (c) [Bz−(MeOH)$_1$−Ar]$^+$ in the visible region. The benzene cation fragment was monitored to measure the spectra.

Though the pickup-type cluster ion source tends to produce the most stable isomer, the ionization process often leaves much internal energy in the cation, and it results in the coexistence of multiple isomers in cases.[4] The attachment of an Ar atom restricts the internal energy of the cluster because of the weak binding energy of Ar (∼500 cm^{-1}), and it is expected to lead to the selective formation of the most stable isomer.[4,23,24] In addition, the weak interaction with the Ar atom is expected to hardly change the electronic structure of the cluster. This has actually been demonstrated in Bz$^+$ and [Bz−(H$_2$O)$_1$]$^+$.[15]

As can be seen from the comparison between panels b and c of Figure 2, the electronic spectrum of [Bz−(MeOH)$_1$]$^+$ remarkably changes upon the attachment of Ar. In the spectrum of [Bz−(MeOH)$_1$−Ar]$^+$, the new absorption below 20 000 cm^{-1} becomes rather stronger, and the C−X (π, π) transition, above 20 000 cm^{-1}, is highly suppressed. This spectral change clearly demonstrates that multiple isomers coexist in [Bz−(MeOH)$_1$]$^+$ and the population ratio among the isomers is changed in [Bz−(MeOH)$_1$−Ar]$^+$. It seems that the preferential production of one of the isomers of [Bz−(MeOH)$_1$−Ar]$^+$ occurs and that isomer has the strong perturbation in the electronic structure of the benzene moiety, resulting in the stronger absorption below 20 000 cm^{-1}.

It has been well established that in the neutral Bz−(MeOH)$_1$ cluster, the methanol molecule locates on the aromatic ring and its OH group is hydrogen-bonded to the π electrons of the benzene moiety.[28] Such a structure cannot be stable in the cluster cation because of the repulsion between the positive charges in the aromatic ring and the hydrogen of the methanol moiety. Instead of the π-hydrogen bond in the neutral cluster, the charge−dipole interaction between the benzene cation and the methanol molecule should be the primary intermolecular interaction in the cluster cation.[4,17] Considering the similarity to [Bz−(H$_2$O)$_1$]$^+$,[8−17] two stable isomers can be assumed for [Bz−(MeOH)$_1$]$^+$; one is the "side" isomer where the methanol moiety locates in the aromatic ring plane bound by the charge−dipole interaction and CH−O hydrogen bonds. The other is the "on-ring" isomer where the methanol moiety places on the top of the aromatic ring and its nonbonding electrons directly face to the positively charged aromatic ring. In this isomer, charge transfer would also contribute to the intermolecular interaction.

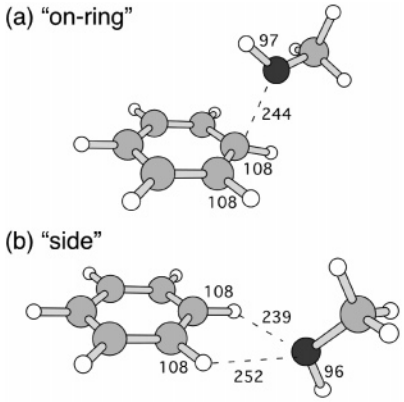

Figure 3. Schematic representation of the (a) on-ring and (b) side isomers of [Bz−(MeOH)$_1$]$^+$ found in the energy optimization at the B3LYP/cc-pVTZ level calculations. Numbers in the figure show selected inter- and intramolecular bond distances in pm.

We carried out the DFT calculations of the stable structures of [Bz−(MeOH)$_1$]$^+$ at the B3LYP/cc-pVTZ level by using the Gaussian 98 program package.[29] As expected in the qualitative discussion described above, two stable structures corresponding to the on-ring and side isomers were actually found in the calculations, and their schematic structures are shown in Figure 3. The binding energy of the cluster was evaluated to be 11.51 and 10.56 kcal/mol for the on-ring and side isomers, respectively, including the zero-point energy (ZPE) corrections. Different from the case of [Bz−(H$_2$O)$_1$]$^+$,[9−12,16,17] the calculations estimated that the on-ring structure is more stable than the side structure by 0.95 kcal/mol.

In the on-ring isomer, the interaction between the hole in the π orbital of the benzene ring and the nonbonding electrons of the methanol moiety would result in the strong perturbation to the electronic structure of the benzene cation site. On the other hand, no remarkable perturbation to the π orbital is expected for the side isomer because the nonbonding electrons and the π orbital are orthogonal to each other. To confirm such a qualitative expectation, we performed time-dependent density functional theory (TDDFT) calculations at the B3LYP/cc-pVTZ level. Electronic transitions of the bare benzene cation and those of the side and on-ring isomers of [Bz−(MeOH)$_1$]$^+$ were calculated on the basis of the optimized geometries in the cation ground state (D_0), and the resultant spectral simulations are shown in Figure 4a−c, respectively. In the visible region, only a (π, π) transition corresponding to the C−X transition is predicted for the bare benzene cation (actually, the B−X transition is also predicted around 22 000 cm^{-1}, but its intensity is estimated to be negligible in the present scale), and no transition is expected, especially in the region below 20 000 cm^{-1}. A very similar spectrum is predicted for the side isomer of [Bz−(MeOH)$_1$]$^+$, indicating the small perturbation to the electronic structure. On the other hand, for the on-ring isomer of [Bz−(MeOH)$_1$]$^+$, a strong transition occurs from the nonbonding electron (n) of the methanol moiety mixed with the π orbital of the benzene moiety to the hole of the π orbital of the benzene moiety. This transition can be regarded as a charge-transfer (CT) transition, and its transition energy is estimated to be at around 15 000 cm^{-1}. This "intermolecular" (n, π) transition well agrees with the newly observed absorption below 20 000 cm^{-1} in the spectra of [Bz−(MeOH)$_1$]$^+$ and [Bz−(MeOH)$_1$−Ar]$^+$. A weaker transition from the delocalized σ orbital of the methanol site (C−H, C−C, and O−H) to the hole of the π orbital of the ring is also predicted at 23 800 cm^{-1}, and the C−X transition is expected to shift to 29 400 cm^{-1} in

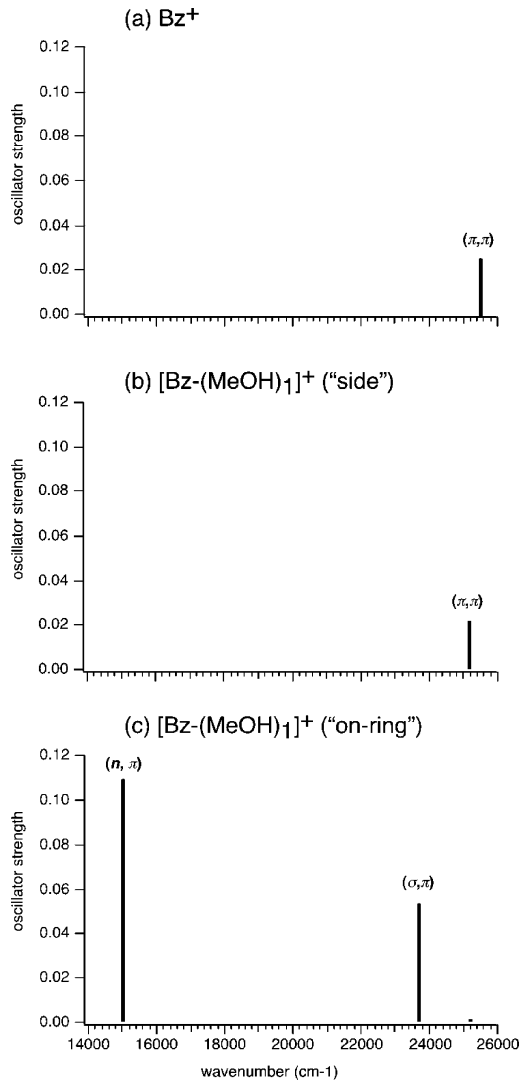

Figure 4. Spectral simulation of the electronic transitions in the visible region of (a) the bare benzene cation, (b) side isomer, and (c) on-ring isomer of $[Bz-(MeOH)_1]^+$ by time-dependent density functional theory (TDDFT) calculations at the B3LYP/cc-pVTZ level.

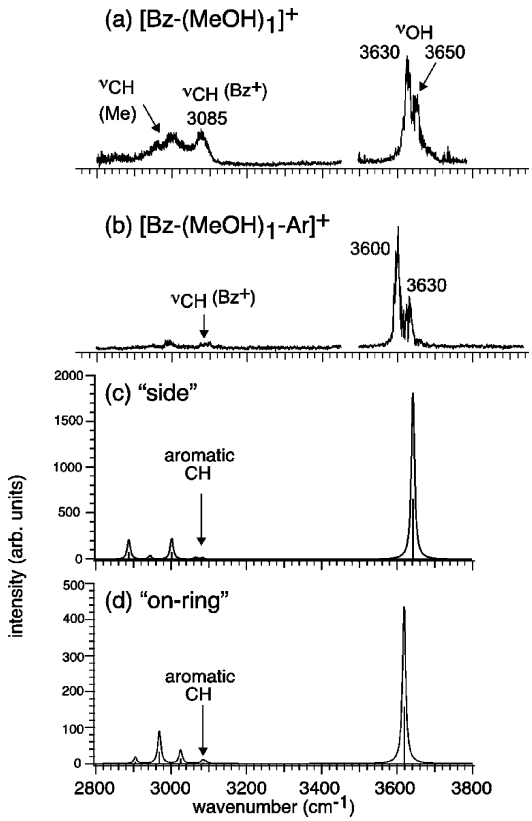

Figure 5. Infrared (IR) spectra of (a) $[Bz-(MeOH)_1]^+$ and (b) $[Bz-(MeOH)_1-Ar]^+$ in the 3 μm region. The benzene cation and $[Bz-(MeOH)_1]^+$ fragments were monitored to measure the spectra, respectively. Simulated IR spectra of $[Bz-(MeOH)_1]^+$ on the basis of the (c) side and (d) on-ring isomers. The calculation level is B3LYP/cc-pVTZ and the scaling factor of 0.96 is applied to the calculated harmonic frequencies. The stick spectra are transformed into the continuous spectra by the convolution with a Lorentzian function of 10 cm^{-1} full width at half-maximum.

the on-ring isomer. These transitions would be responsible for the long tail to the high-frequency side in the spectrum of $[Bz-(MeOH)_1-Ar]^+$.

On the basis of these calculations, the spectral change of $[Bz-(MeOH)_1]^+$ upon the attachment of Ar is well explained by the coexistence of the isomers. Both the on-ring and side isomers contribute to the spectrum of $[Bz-(MeOH)_1]^+$. Because the absorption below 20 000 cm^{-1}, which is attributed to the intermolecular (n, π) transition, only occurs in the on-ring isomer, the population of the side isomer suppresses the absorption intensity below 20 000 cm^{-1} relative to that above 20 000 cm^{-1} from the (π, π) and (σ, π) transitions. On the other hand, the observed spectrum of $[Bz-(MeOH)_1-Ar]^+$ is well reproduced by the spectral simulation of the on-ring isomer. It means that the preferential formation of the on-ring isomer occurs upon the attachment of Ar.

The above discussion is still qualitative, and we should note that the relative band intensities in the observed spectrum of $[Bz-(MeOH)_1]^+$ are not straightforward. Because the (n, π) transition of the on-ring isomer is predicted to be much stronger than the (π, π) and (σ, π) transitions, the weaker absorption below 20 000 cm^{-1} in the observed spectrum of $[Bz-(MeOH)_1]^+$ might mean that population of the more stable on-ring isomer is much lower than that of the less stable side isomer. This discrepancy cannot be clearly explained at the present stage. It is, however, worthwhile to note that the energy difference between two isomers is quite small (0.95 kcal/mol), and in such a case, the more stable isomer does not necessarily populate more than less stable isomer because of the entropy (state density) factor, when the clusters are hot. Moreover, the quantitative reliability of transition intensities in TDDFT calculations has not yet been fully established.

To support the above discussion on the electronic spectra and obtain more detailed information on the cluster structure, we carried out IR spectroscopy of $[Bz-(MeOH)_1]^+$. Figure 5a shows the IR spectrum of $[Bz-(MeOH)_1]^+$ in the 3 μm region. A gap in the spectrum around 3500 cm^{-1} is the result of the lack of IR output power caused by the absorption of the impurity water in the DFM crystal. The OH stretch band of the methanol moiety appears with two peaks at 3630 and 3650 cm^{-1}. Their frequency shifts from that of the bare methanol monomer (ν_1, 3681 cm^{-1}) are 51 and 31 cm^{-1}, respectively. [30] The small frequency shifts indicate that the OH group of the methanol moiety is free from a hydrogen bond. The magnitude of the shifts is quite similar to that of $[Bz-(H_2O)_1]^+$, in which the water moiety is free from the hydrogen bond.[11−13,16,17] In the CH stretching vibrational region, two bands are seen, and they are assigned by comparison with the IR spectra of the benzene cation and methanol monomers as follows:[30−32] the 3085 cm^{-1} band is from the aromatic CH stretch of the benzene cation moiety (ν_{20}, 3090 cm^{-1} in the monomer cation), the 3000 cm^{-1}

band is an overlap of the ν_2 and ν_9 bands of the methanol moiety (3000 and 2960 cm^{-1} in the methanol monomer, respectively), and a weak bump at around 2850 cm^{-1} would be attributed to the ν_3 band of the methanol moiety (2844 cm^{-1} in the monomer). The frequency shifts of these CH stretches upon cluster formation are almost negligible. The present spectrum is essentially the same as that previously reported by Solcà and Dopfer,[17] but the signal-to-noise ratio of the present spectrum is much better especially in the CH stretch region.

The electronic spectroscopy indicates the coexistence of the on-ring and side isomers for [Bz−(MeOH)$_1$]$^+$. In both the isomers, the OH group of the methanol moiety is free from a hydrogen bond, and it cannot be a sufficient spectral signature to determine an unambiguous structure. The intensity enhancement of the aromatic CH stretch band would be a key factor for the cluster structure analysis. IR transition intensities of aromatic CH stretches of a bare molecular cation are substantially weaker than those of the OH and alkyl CH stretch bands.[32−34] Then, as far as perturbations occur on the aromatic ring, the CH stretch bands continue to be weak. On the other hand, the direct intermolecular interaction to the CH bond, such as CH−O hydrogen bond formation, substantially enhances the CH stretch band intensity. The typical example was seen in [Bz−(H$_2$O)$_1$]$^+$. The intensity of the aromatic CH stretch band of [Bz−(H$_2$O)$_1$]$^+$ was found to be as strong as those of the OH stretches, representing that the side structure is feasible for the stable form.[11−13] DFT calculations also confirmed that the side form is more stable than the on-ring structure.[8−12,16,17] Because the previous study of [Bz−(MeOH)$_1$]$^+$ by Solcà and Dopfer separately measured the OH and CH stretch regions, it was difficult to compare the relative intensities of the OH and aromatic CH stretches.[17] In the present measurement, the continuous scan over the whole 3 μm region enables us to compare the OH and CH stretch band intensities. The present IR spectrum shows that the aromatic CH band intensity is almost half of that of the OH stretch, and such a strong aromatic CH stretch intensity suggests the contribution of the side structure of [Bz−(MeOH)$_1$]$^+$. Though the coexistence of the on-ring isomer is indicated by electronic spectroscopy, the contribution of the on-ring isomer to the IR spectrum is unclear.

Then, IR spectroscopy of [Bz−(MeOH)$_1$−Ar]$^+$ was also carried out to examine the effect of the preferential formation of the on-ring isomer suggested by the electronic spectroscopy. The IR spectrum of [Bz−(MeOH)$_1$−Ar]$^+$ is shown in Figure 5b. This spectrum was measured by monitoring the [Bz−(MeOH)$_1$]$^+$ fragment, and no benzene cation fragment was observed even upon the free OH stretch band excitation (3600 cm^{-1}). On the basis of the same analysis as that applied to [Bz−(H$_2$O)$_1$]$^+$,[13] the absence of the benzene cation fragment shows that the binding energy between the benzene cation and methanol moieties is larger than 3600 cm^{-1} (10.3 kcal/mol). This is consistent with the binding energy estimation by the B3LYP/cc-pVTZ calculations described in the previous subsection (11.51 and 10.56 kcal/mol for the on-ring and side isomers, respectively). These values are slightly larger than the binding energy of [Bz−(H$_2$O)$_1$]$^+$, which has been experimentally determined to be 9.40 ± 0.34 kcal/mol.[7,8,13]

Spectral changes upon the attachment of Ar are also drastic in the IR spectrum; the intensities of all the CH stretch bands are remarkably reduced. Because the vibrational energy of ~3000 cm^{-1} is large enough for the evaporation of the Ar atom, the intensity reduction of the aromatic CH bands in the IR spectrum should not be the result of the reduction of the dissociation yield but should be attributed to the reduction of the IR transition intensities of the isomer cluster, which is cooled by the attachment of Ar. When the analogy with [Bz−(H$_2$O)$_1$]$^+$ is considered, it is quite reasonable to expect that only the side-type isomer shows a remarkable enhancement of the IR intensity of the aromatic CH stretch band, while the on-ring-type isomer has no remarkable perturbation to the aromatic CH stretch and its IR intensity is weak. Then, the reduction of the aromatic CH stretch band in the spectrum of the Ar cluster is consistent with the preferential formation of the on-ring isomer, which was also demonstrated by electronic spectroscopy.

Not only the aromatic CH stretch band but also the CH stretches of the methanol moiety are also weakened upon the Ar attachment. This might be interpreted as the CH stretches of the methanol moiety in the side isomer being largely enhanced by the intensity borrowing from the strong aromatic CH stretch and the suppression of the side isomer production upon the Ar attachment also resulting in the reduction of the CH stretch intensity of the methanol moiety. However, strong coupling between the CH stretches of the methanol and benzene moieties is normally unlikely, and this interpretation is tentative.

We carried out the simulations of the IR spectra on the basis of the calculated structures of the side and on-ring isomers of [Bz−(MeOH)$_1$]$^+$ at the B3LYP/cc-pVTZ level. The simulated spectra in the OH and CH stretch regions are shown in Figure 5c and d. It should be noted that the intensities of these two spectra are shown in different scales to represent the relative intensities between the OH and CH stretches in each spectrum. A scaling factor of 0.96 was applied to the calculated harmonic frequencies. This scaling factor is determined to reproduce the CH stretch frequency of the bare benzene cation. The calculated spectral features are quite similar between these two simulations. No remarkable enhancement of the aromatic CH stretch intensity is found in the simulation on the basis of the side isomer, although the same level of calculations predicted a remarkable enhancement of the aromatic CH stretch for the similar side isomer of [Bz−(H$_2$O)$_1$]$^+$.[11,12] The strong appearance of the aromatic CH stretch in the observed spectrum of [Bz−(MeOH)$_1$]$^+$ cannot be reproduced by the DFT calculations, and the origin of the failure of the simulation is unclear at present. As was qualitatively described above, the change of the IR spectral features upon the Ar attachment is reasonably explained by the coexistence of the on-ring and side isomers, but the spectral simulations are not helpful for the isomer assignments of [Bz−(MeOH)$_1$]$^+$.

In addition to the spectral change upon the Ar attachment, an alternative IR spectral signature of the coexistence of the on-ring and side isomers is the splitting of the free OH stretch band in [Bz−(MeOH)$_1$]$^+$. A small frequency difference (25 cm^{-1}) of the free OH stretch band is predicted by the DFT calculations as seen in Figure 5c and d, and it fits the observed splitting (~20 cm^{-1}) well. The lower-frequency OH band (3630 cm^{-1}) is tentatively assigned to the free OH of the on-ring isomer, and the higher-frequency band (3650 cm^{-1}) is assigned to the side isomer. In the IR spectrum of [Bz−(MeOH)$_1$−Ar]$^+$, two OH stretch bands appear at 3600 and 3630 cm^{-1}. Because the preferential production of the on-ring isomer is suggested from the intensity reduction of the aromatic CH stretch, as well as from the results of the electronic spectroscopy, this splitting of the OH stretch band can be attributed to the difference of the Ar attachment sites. When the methanol occupies one side of the aromatic ring and the Ar atom attaches on the other side, no frequency shift of the OH stretch may occur. This would be the case for the 3630 cm^{-1} band, which is the same frequency as the on-ring isomer band observed in [Bz−(MeOH)$_1$]$^+$. On

the other hand, when the Ar atom is hydrogen-bonded to the OH group of the methanol site, it would cause a low-frequency shift of a few tens of cm^{-1}.[4,24] The 3600 cm^{-1} band seems to be reasonably attributed to this case.

The present electronic and IR spectroscopic study demonstrated that the on-ring and side isomers coexist in the prepared $[Bz-(MeOH)_1]^+$ clusters, and the on-ring isomer, which is slightly more stable than the side isomer in the DFT calculations, is preferentially produced in $[Bz-(MeOH)_1-Ar]^+$. This result is quite different from that of $[Bz-(H_2O)_1]^+$, which prefers the side structure.[9−12,16,17] A similar on-ring structure was theoretically predicted for $[Bz-(NH_3)_1]^+$, although it has not yet been experimentally confirmed.[35,36] Moreover, the formation a covalent bond between the aromatic carbon and ammonia nitrogen atoms was also pointed out for $[Bz-(NH_3)_1]^+$, which can be regarded as a reaction intermediate in nucleophilic substitution reactions.[36] In the case of $[Bz-(MeOH)_1]^+$, the intermolecular C−O distance is estimated to be 244 pm by the present B3LYP/cc-pVTZ calculations. This is much longer than the C−N distance theoretically predicted for $[Bz-(NH_3)_1]^+$ (163 pm at the B3LYP/6-311G (d, p) level),[36] and the covalent bond formation may not occur in $[Bz-(MeOH)_1]^+$.

Ammonia and methanol have larger proton affinities (204 and 180 kcal/mol, respectively) than water (165 kcal/mol).[21] The proton affinity can be regarded as an index of the electron donating ability of the solvent molecule. In the case of the on-ring isomer, not only the electrostatic (charge-dipole) interaction but also the charge-transfer interaction from the n orbital of the solvent molecule to the hole of the π orbital of the benzene ring would be important. On the other hand, no such direct interaction exists between the n and π orbitals in the side isomer. An increase of the proton affinity (i.e., electron donating ability) enhances the charge-transfer interaction, and it causes the advantage of the on-ring isomer over the side isomer. In addition, the smaller dipole moments of ammonia and methanol (1.471 and 1.7 D, respectively) than that of water (1.854 D) also enhances the relative importance of the charge-transfer interaction over the charge-dipole interaction.[22] Thus, the most stable structure changes from the side-type in the cluster with water to the on-ring-type in the clusters with methanol and ammonia.

3. Structure of the $n = 2$ Cluster. To examine the structure of the $n = 2$ cluster, IR spectroscopy was more informative than electronic spectroscopy. Then, we first introduce the results of IR spectroscopy. The IR spectra of $[Bz-(MeOH)_2]^+$ and $[Bz-(MeOH)_2-Ar]^+$ in the 3 μm region are shown in Figure 6a and b, respectively. In the spectrum of $[Bz-(MeOH)_2]^+$, the free OH stretch band appears at 3670 cm^{-1} and an extremely broadened absorption is seen in the 2800−3600 cm^{-1} region. This broad absorption is clearly attributed to the hydrogen-bonded OH stretch of the methanol moiety, and it indicates that the $n = 2$ cluster is formed by the addition of one more methanol molecule to the on-ring or side isomer of $n = 1$ with a hydrogen bond between the methanol molecules (hereafter, we call such structures of $n = 2$ the "hydrogen-bonded" type). The CH stretch region is buried in a long tail of the strong absorption of the hydrogen-bonded OH stretch, and no clear bands are seen. This spectrum is very similar to that of $[Bz-(H_2O)_2]^+$,[11] although the broadening of the spectrum is more significant in $[Bz-(MeOH)_2]^+$, reflecting the stronger hydrogen bond strength. On the other hand, in the spectrum of $[Bz-(MeOH)_2-Ar]^+$, of which the internal energy should be much lower, the hydrogen-bonded OH band completely disappears. The CH stretch bands are also hardly seen, and the free OH stretch band only remains

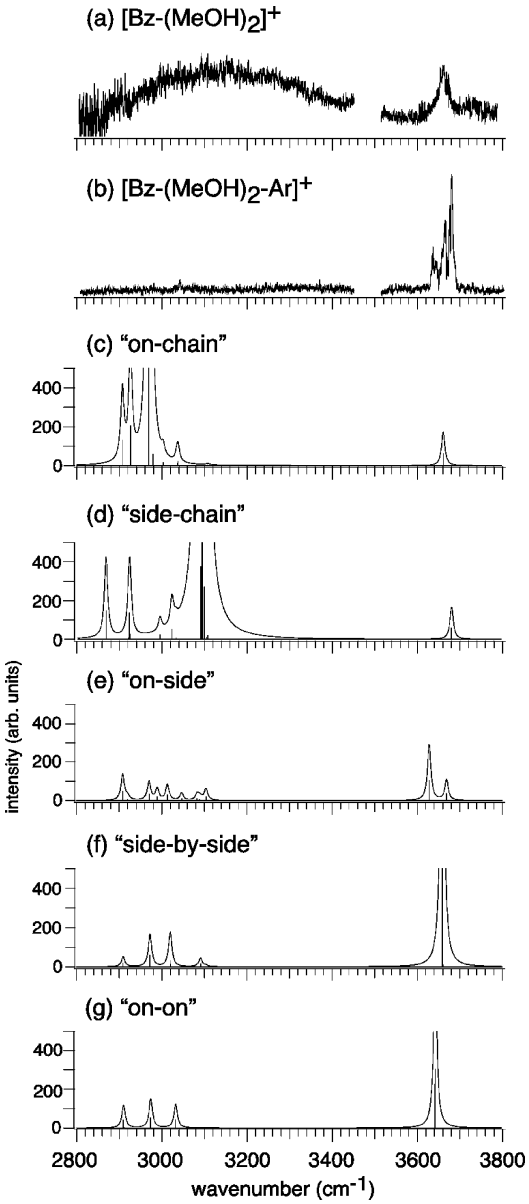

Figure 6. Infrared (IR) spectra of (a) $[Bz-(MeOH)_2]^+$ and (b) $[Bz-(MeOH)_2-Ar]^+$ in the 3 μm region. The $[Bz-(MeOH)_1]^+$ and $[Bz-(MeOH)_2]^+$ fragments were monitored to measure the spectra, respectively. Simulated IR spectra of $[Bz-(MeOH)_2]^+$ of the (c) on-chain, (d) side-chain, (e) on-side, (f) side-by-side, and (g) on-on isomers. The calculation level is B3LYP/6-31G(d, p), and the scaling factor of 0.96 is applied to the calculated harmonic frequencies. The stick spectra are transformed into the continuous spectra by the convolution with a Lorentzian function of 10 cm^{-1} full width at half-maximum.

in the spectrum with small splittings. Disappearance of the hydrogen-bonded OH stretch band means that the two methanol molecules separately solvate the benzene cation moiety without forming the methanol dimer subunit (we call such structures of $n = 2$ the "separate" type). The absence of the aromatic CH stretch band would mean that both the methanol molecules locate on the aromatic ring.

Such a drastic change of the IR spectrum upon the attachment of the Ar atom to $[Bz-(MeOH)_2]^+$ suggests a similar conclusion to that of the $n = 1$ cluster: multiple isomers (i.e., hydrogen-bonded and separate types) contribute to the IR spectrum of $[Bz-(MeOH)_2]^+$, but the attachment of Ar leads to the preferential production of the separate type. We carried out DFT calculations to examine such an experimental suggestion. Because of the limitation of our computation resources, we

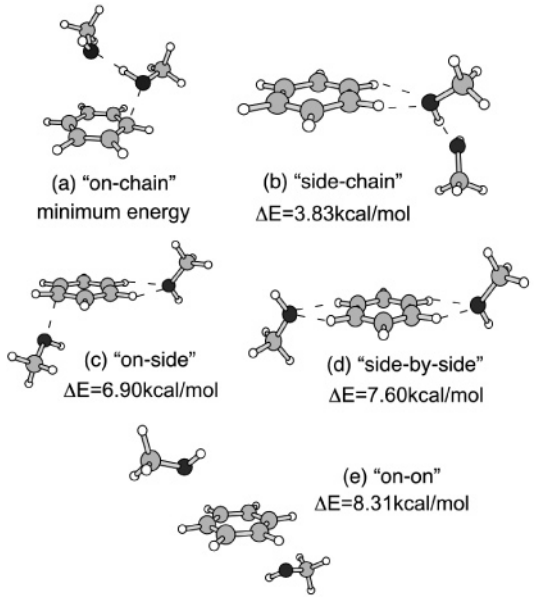

Figure 7. Schematic representation of the stable structures of [Bz−(MeOH)$_2$]$^+$ in the B3LYP/6-31G (d, p) level. The relative energies include the zero-point energy (ZPE) corrections.

employed the B3LYP/6-31G(d, p) level for the calculations of the n = 2 cluster. As in the case of [Bz−(H$_2$O)$_2$]$^+$,[8,12] many stable structural isomers were found for the DFT calculations of [Bz−(MeOH)$_2$]$^+$, and they were finally categorized to 5 types. A schematic representation of these isomer structures is shown in Figure 7 with the relative energies including the ZPE corrections. The vibrational spectrum simulation on the basis of the representative isomer of each type is shown in Figure 6c−g. The hydrogen-bonded methanol dimer subunit can locate either on the ring or at the side of the ring, and it results in the "on-chain" or "side-chain", respectively, isomers of the hydrogen-bonded type. In the case of the separate type, three different types, "on-on", "side-by-side", and "on-side", corresponding to the interaction sites with two independent methanol molecules, were found in the calculations. Each type of isomer has several variations with respect to the relative conformation of the methanol moiety and the choice of the interaction sites. All the initial structures in which both methanol molecules locate on the same side of the aromatic ring plane finally converged to the on-chain isomer during the geometry optimization, and the on-on type was restricted to have one methanol molecule in each side of the ring plane.

The spectral simulation on the basis of the side-chain isomer reproduces the spectral features, especially the hydrogen-bonded OH stretch band, of the observed spectrum of [Bz−(MeOH)$_2$]$^+$ well. However, the most stable isomer is estimated to be the on-chain isomer in the B3LYP/6−31G(d, p) calculation. The free OH stretch band is better reproduced in this isomer, while the low-frequency shift of the hydrogen-bonded OH stretch band is overestimated. The energy difference between these two isomers is 3.83 kcal/mol, and the unequivocal determination of the structure of the hydrogen-bonded-type isomer seems to be difficult only on the basis of the IR spectrum and DFT calculations.

The IR spectrum of [Bz−(MeOH)$_2$−Ar]$^+$ clearly demonstrates that the separate-type isomer is preferentially produced with the Ar attachment. With the DFT calculations, all of the separate-type isomers are predicted to show very similar IR spectra. Only the free OH stretch of the methanol moiety has a strong IR intensity with a small shift of its frequency, and it well reproduces the observed feature of [Bz−(MeOH)$_2$−Ar]$^+$. Similar to the case of the n = 1 cluster, no enhancement of the aromatic CH stretch intensity was predicted for the CH−O hydrogen bond formation even in the side-by-side and on-side isomers, although the disappearance of the aromatic CH stretch band in the observed spectrum can be qualitatively explained by the preference of the on-on isomer, with the analogy to the n = 1 cluster. However, the small energy differences among the separate-type isomers and the observed splitting of the free OH stretch band would suggest the possibility of the coexistence of several separate-type isomers in [Bz−(MeOH)$_2$−Ar]$^+$. The splitting of the free OH stretch band can also be attributed to multiple sites for the Ar attachment. The lack of clear spectral fingerprints and many plausible candidates prevent us from making an unequivocal determination of the structure of the separate-type cluster as being responsible for the observed spectrum of [Bz−(MeOH)$_2$−Ar]$^+$.

The Ar attachment has been known to discriminate less stable isomers because of the weak binding energy with the Ar atom. The preferential production of the separate-type isomers of [Bz−(MeOH)$_2$−Ar]$^+$ suggests that the separate type might be more stable than the hydrogen-bonded type. The DFT calculations, however, predicted that all of the separate-type isomers are much less stable than the hydrogen-bonded-type isomers (ΔE = 6.9−8.31 kcal/mol), and this conclusion conflicts with the suggestion of the experimental spectra. A limitation of the theory in the energy evaluation is one of the plausible explanations for this discrepancy. The [Bz−(MeOH)$_n$]$^+$ clusters are open shell systems, and the reliability of the B3LYP functional to evaluate the stabilization energies of such open shell systems has not yet been extensively confirmed, especially for clusters larger than dimers. However, the B3LYP/6-31G(d, p) level calculation of the stabilization energy of [Bz−(H$_2$O)$_1$]$^+$ showed a very good agreement (within 0.34 kcal/mol) with the experimental value,[13] and we have no strong evidence for failure of this level of calculation for [Bz−(MeOH)$_2$]$^+$. An alternative and more plausible possibility is that the Ar attachment itself causes a selective stabilization or preference of the separate-type isomer. When the on-on- or on-side-type isomer is formed, the acidity of the methanol molecule locating on the ring would be significantly enhanced because of the partial charge transfer into the hole of the π orbital. This is reflected in the larger energy difference between the on-chain and side-chain isomers of n = 2 (3.83 kcal/mol) than that between the on-ring and side isomers of n = 1 (0.95 kcal/mol). Such enhancement of the acidity of the free OH site is reduced in the terminal methanol in the hydrogen-bonded-type because of the larger separation from the charge. When the Ar atom is bound to the free OH site of the clusters, the interaction with Ar is expected to be stronger in the separated type than in the hydrogen-bonded type. Therefore, it can cause the preferential production of the separate type over the hydrogen-bonded type in [Bz−(MeOH)$_2$−Ar]$^+$, even though the hydrogen-bonded type is much more stable the separate type in [Bz−(MeOH)$_2$]$^+$. At the present stage, however, the origin of this discrepancy is still ambiguous, and both the interpretations of the discrepancy have no firm evidence. It is difficult to determine the most stable isomer of [Bz−(MeOH)$_2$]$^+$ on the basis of the infrared spectra and DFT calculations.

As can be seen in the n = 1 cluster, electronic spectroscopy of the benzene moiety is a powerful method to distinguish the on-ring-type isomer from the side-type isomer. We carried out electronic spectroscopy of [Bz−(MeOH)$_2$]$^+$ for further characterization of the structure of the n = 2 cluster. Figure 8a and b shows the electronic spectra of [Bz−(MeOH)$_2$]$^+$ and [Bz−

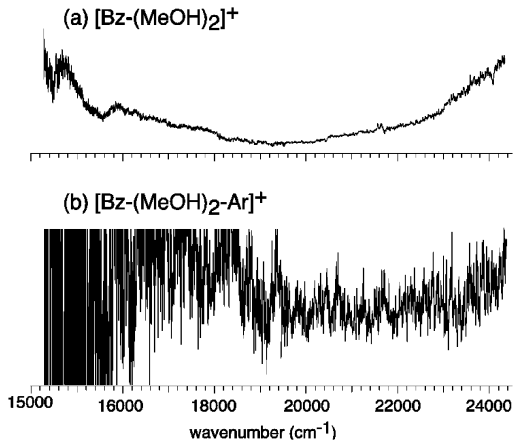

Figure 8. Electronic spectra of (a) $[Bz-(MeOH)_2]^+$ and (b) $[Bz-(MeOH)_2-Ar]^+$. The benzene cation fragment was monitored to measure the spectra.

$(MeOH)_2-Ar]^+$, respectively. In the spectrum of $[Bz-(MeOH)_2]^+$, not only the C−X (π, π) transition of the benzene cation moiety but also the intermolecular (n, π) transition strongly appear in the region above and below 20 000 cm^{-1}, respectively. The latter transition occurs only in isomers having the on-ring-type interaction (on-chain, on-on, and on-side). As expected from the TDDFT calculations of $n = 1$, the intensity of the (n, π) transition below 20 000 cm^{-1} would be much stronger than that of the (π, π) or (σ, π) transitions above 20 000 cm^{-1}. The almost even intensity of the two transitions in the spectrum of $[Bz-(MeOH)_2]^+$ suggests that not only the on-ring-type isomers but also the side-type isomers (side-chain and side-by-side) contribute to the spectrum. Then, coexistence of at least two different types of isomers with respect to the interaction site is concluded for $[Bz-(MeOH)_2]^+$.

The electronic spectrum of $[Bz-(MeOH)_2-Ar]^+$ only shows a poor signal-to-noise ratio, and it becomes worse especially in the low-energy region because of the laser-power normalization procedure. However, the presence of both the (n, π) and (π, π) (and (σ, π)) absorption bands are seen in the spectrum. In contrast with the case of the $n = 1$ cluster, no remarkable change upon the attachment of Ar occurs in $n = 2$. Under the same cluster preparation condition, the IR spectrum of $[Bz-(MeOH)_2-Ar]^+$ shows no hydrogen-bonded OH stretch band, representing the preferential formation of the separate-type isomers with Ar attachment. The presence of the (n, π) band shows that the side-by-side or on-side isomer contributes to the spectrum, in addition to the on-on isomer suggested by the IR spectrum. The on-side isomer is estimated to be the most stable among the separate-type isomers for $n = 2$. However, the energy differences among the separate-type isomers are very small ($\leq$1.41 kcal/mol), and the coexistence of several separate-type isomers would be quite possible.

In conclusion of the structure of the $n = 2$ cluster, the coexistence of the hydrogen-bonded- and separate-type isomers was shown on the basis of the IR spectra. The attachment of Ar to the cluster results in the remarkably preferential production of the separate-type isomer over the hydrogen-bonded type, although the DFT calculations predicted that the hydrogen-bonded type is much more stable than the separate type. The selective stabilization of the separate-type isomers by Ar attachment was proposed for this discrepancy. The electronic spectra of the cluster cation also indicated the coexistence of the on-ring- and side-type isomers. Unequivocal determination of the isomer structure is very difficult at the present stage because of the small energy differences among the isomers and the discrepancy between the Ar attachment experiment and theoretical predictions.

4. Intracluster Proton and Electron-Transfer Reactions in the Larger Clusters. The IR spectra of the larger $[Bz-(MeOH)_n]^+$ ($n = 3-6$) clusters are shown in Figure 9a. The free OH stretch band forms a single peak, and it shows a gradual high-frequency shift and intensity reduction with increase of the cluster size. Such a feature seems to represent the separation between the charged site and the free OH site. The hydrogen-bonded OH stretch band appears as an extremely broadened absorption in the region of 2800−3500 cm^{-1}, and it indicates the presence of hydrogen-bonded methanol subunits in the clusters. For $n = 5$ and $n = 6$, some band features appear at ~3250 and ~3350 cm^{-1}, respectively, although no remarkable structure is seen in the broadened absorption up to $n = 4$. The alkyl CH stretches of the methanol moiety show no remarkable change with the cluster size, and the aromatic CH stretch band would not be observed because of the interference of the intense hydrogen-bonded OH stretch band. In Figure 9b, IR spectra of the protonated methanol cluster cations, $[MeOH-H^+(MeOH)_n]$, which have recently been reported, are also reproduced.[37,38] When two IR spectra of the same size (n) are compared, a remarkable similarity between the spectra is found in $n \geq 5$, especially on the hydrogen-bonded and free OH stretch bands (the similarity seen in $n = 3$ might be accidental because the spectra of $n = 4$ show clear difference).

In $[Bz-(MeOH)_n]^+$, the gross proton affinity of the methanol moiety increases with the cluster size because of the cooperative effects of the hydrogen bond network. Such an enhancement

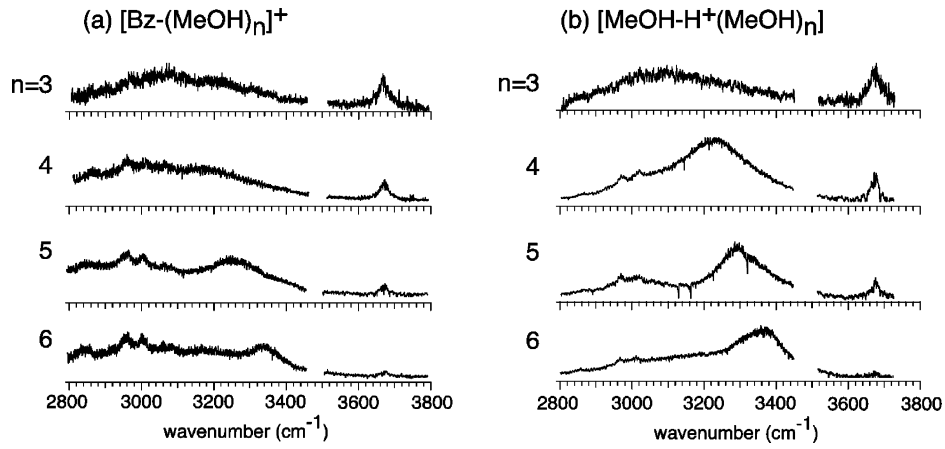

Figure 9. Comparison between the IR spectra of (a) $[Bz-(MeOH)_n]^+$ ($n = 3-6$) and (b) $[MeOH-H^+(MeOH)_n]$ ($n = 3-6$) in the 3 μm region.

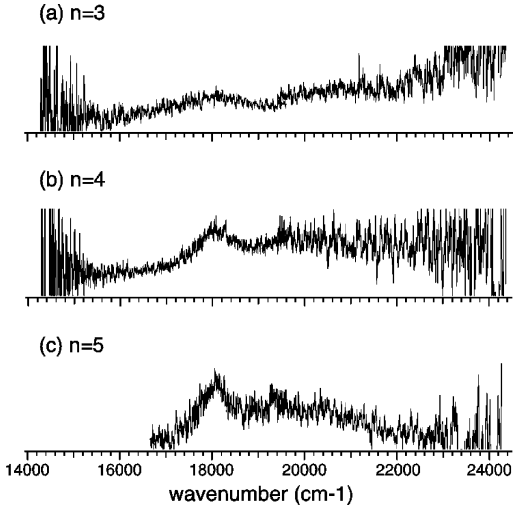

Figure 10. Electronic spectra of [Bz−(MeOH)$_n$]$^+$ (n = 3−5). The benzene cation fragment was monitored to measure the spectra of n = 3, and the (n − 3) fragment cluster cations were monitored in the spectra of n = 4 and 5.

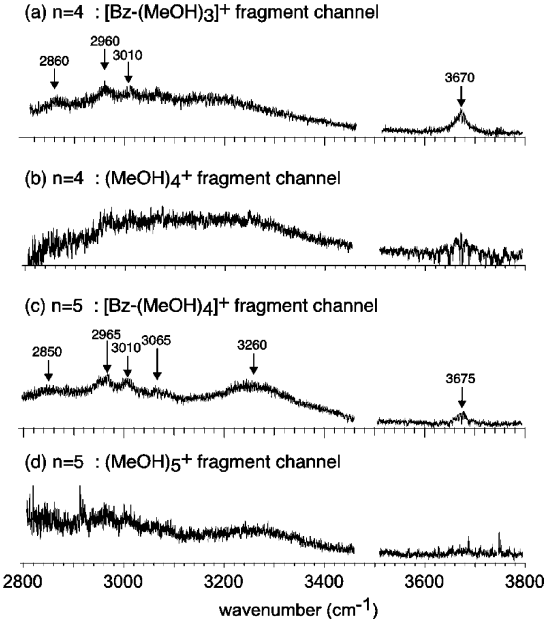

Figure 11. Comparison of the IR spectra of [Bz−(MeOH)$_n$]$^+$ measured by monitoring the (n − 1) fragment and the (MeOH)$_n^+$ fragment, the spectra of n = 4 by monitoring the (a) [Bz−(MeOH)$_3$]$^+$ and (b) (MeOH)$_4^+$ fragments, the spectra of n = 5 by monitoring the (c) [Bz−(MeOH)$_4$]$^+$ and (d) (MeOH)$_5^+$ fragments.

of the proton affinity may finally cause an intracluster proton transfer from the benzene cation moiety to the methanol moiety. Then, the similarity between the IR spectra of [Bz−(MeOH)$_n$]$^+$ and [MeOH−H$^+$(MeOH)$_n$] in $n \geq 5$ is well interpreted in terms of the intracluster proton transfer to form the phenyl radical-protonated methanol clusters ([C$_6$H$_5$−H$^+$(MeOH)$_n$]), where the phenyl radical plays a compatible role with a methanol molecule in [MeOH−H$^+$(MeOH)$_n$].

Another signature of the intracluster proton transfer in $n \geq 5$ is seen in the electronic spectra of [Bz−(MeOH)$_n$]$^+$ (n = 3−5), shown in Figure 10. The electronic spectrum of n = 6 unfortunately could not be observed because of the weak signal intensity. Although the quality of these spectra is worse than that of n = 1, the spectral feature can be seen. The intermolecular (n, π) transition is hardly seen in $n \geq 3$, and the C−X (π, π) transition is the main feature in n = 3 and 4. A new feature appears around 18 000 cm^{-1} in $n \geq 3$ and 4, and it becomes the main feature in n = 5 accompanied by the disappearance of the C−X transition. When the proton transfer occurs, the electronic structure of the aromatic moiety is drastically changed from the benzene cation to the neutral phenyl radical.[15] The electronic transition of phenyl radical is very weak in the region of <40 000 cm^{-1}, and only the $^2B_1 \leftarrow {}^2A_1$ transition has been found around 19 000 cm^{-1}.[39] The disappearance of the C−X transition and the appearance of the new absorption agree well with the change of the electronic structure of the aromatic ring associating with the intracluster proton transfer. The weak appearance of the 18 000 cm^{-1} band in the n = 3 and 4 clusters would result from the proton transfer beyond the potential barrier because of the high internal energy component.

A similar intracluster proton-transfer reaction has been confirmed for [Bz−(H$_2$O)$_n$]$^+$ in $n \geq 4$ on the basis of the signature in the IR and electronic spectra.[12,14,15] The observed threshold size of the proton transfer in [Bz−(MeOH)$_n$]$^+$ is n = 5, and it is larger than that of [Bz−(H$_2$O)$_n$]$^+$ despite the larger proton affinity of bare methanol than water. A large cooperative effect is required to extract the proton from the benzene cation because the phenyl radical has a much higher proton affinity (214 kcal/mol) than that of bare water or methanol.[40] Although the size dependence of the proton affinity of small water clusters, (H$_2$O)$_n$, has been extensively studied,[15,21] such a study on methanol clusters is more scarce. If the magnitude of the cooperative effect is smaller in methanol than water, it would cause the higher threshold of the intracluster proton-transfer reaction. Mass spectrometric studies demonstrated the presence of the potential barrier for the intracluster proton-transfer reaction of [Bz−(H$_2$O)$_n$]$^+$ and the importance of the internal energy factor.[7,8] Although a similar magnitude is expected for the internal energy of [Bz−(MeOH)$_n$]$^+$ in the present study and that of [Bz−(H$_2$O)$_n$]$^+$ in our previous study, the difference of the barrier height can be an alternative explanation of the larger threshold size in [Bz−(MeOH)$_n$]$^+$.

In addition to the intracluster proton-transfer reaction, an experimental evidence for another intracluster reaction was found in the large clusters. Not only the fragmentation to [Bz−(MeOH)$_{n-1}$]$^+$ (from the evaporation of a methanol molecule) but also to (MeOH)$_n^+$ was found, associating with the IR vibrational excitation of the [Bz−(MeOH)$_n$]$^+$ ($n \geq 4$) clusters. The latter fragment is the result of a minor channel, and its yield is lower than 10% of that of the former channel. The production of the nonprotonated (MeOH)$_n^+$ fragment, however, strongly suggests that the intracluster electron-transfer (charge-transfer) reaction occurs to form the [Bz−(MeOH)$_n^+$]-type cluster prior to the vibrational predissociation. Zwier and co-workers have reported the production of (MeOH)$_n^+$ as a minor channel in REMPI of the neutral Bz−(MeOH)$_n$ clusters ($n \geq$ 3), although its detailed mechanism has not yet been clarified.[25] Figure 11b and d shows the IR spectra of [Bz−(MeOH)$_n$]$^+$ (n = 4 and 5, respectively) by monitoring the (MeOH)$_n^+$ fragment channels. For the n = 6 clusters, the (MeOH)$_6^+$ fragment channel could not be confirmed. The IR spectra measured by the major [Bz−(MeOH)$_{n-1}$]$^+$ channel were also reproduced in Figure 11a and c for comparison. In each of the n = 4 and 5 clusters, the two IR spectra by the monitoring the different dissociation channels show similar spectral features. These results suggest that the difference of the dissociation channel is not the result of the presence of the [Bz−(MeOH)$_n^+$]-type isomer in the ground state but the intracluster electron-transfer reactions occurring in the vibrationally excited state. We also observed the (MeOH)$_3^+$ production upon the electronic excita-

tion of $[Bz-(MeOH)_4]^+$ and $[Bz-(MeOH)_5]^+$ in the visible region. However, the signal intensity was so weak that the electronic spectra for this channel could not be measured.

IV. Summary

In the present work, we carried out IR and electronic spectroscopy of $[Bz-(MeOH)_n]^+$ ($n = 1-6$), and the microsolvation structure of the benzene cation with methanol was studied. The structures of the $n = 1$ and 2 clusters were also examined by the DFT calculations. The coexistence of the multiple isomers was confirmed for $n = 1$ and 2. The isomer discrimination was carried out by the Ar attachment, and the preferential production of the on-ring- and separate-type isomers was found for $n = 1$ and $n = 2$, respectively. The DFT calculation suggested that the on-ring isomer is the most stable in $n = 1$, and this is in contrast with the case of $[Bz-(H_2O)_n]^+$, where the most stable isomer is the side type. The change of the most stable isomer structure was discussed in terms of the competition between the charge−dipole and charge-transfer interactions. On the other hand, the DFT calculations of $n = 2$ predicted that the hydrogen-bonded type is much more stable than the separate type, and it conflicted with the implication of the Ar attachment. The selective stabilization of the separate isomers by Ar attachment was proposed as a plausible origin of the discrepancy. The unequivocal determination of the most stable structure of the $n = 2$ cluster was difficult. The spectroscopic signatures of the intracluster proton-transfer reaction were found for the $n \geq 5$ clusters. The origin of the higher threshold of the reaction than that in $[Bz-(H_2O)_n]^+$ was discussed. The evidence for intracluster electron-transfer reaction also found for $[Bz\text{-}(MeOH)_n]^+$ ($n \geq 4$), and the IR spectroscopy indicated that the reaction occurs in the vibrationally excited state.

Acknowledgment. The authors thank Prof. T. Ebata in Hiroshima University, Prof. H. Ishikawa in Kobe University, and Dr. T. Maeyama in Tohoku University for their valuable discussions. This work was partially supported by MEXT Japan through a project (No. 16002006) of the Grant-in-Aid for specifically promoted research.

References and Notes

(1) *Ion and Cluster Ion Spectroscopy and Structure*; Maier, J. P., Ed.; Elsevier: Amsterdam, 1989.
(2) *Clusters of Atoms and Molecules II*; Harberland, H., Ed.; Springer-Verlag: Berlin, 1994
(3) Meot-Ner (Mautner), M. *Chem. Rev.* **2005**, *105*, 213.
(4) Dopfer, O. *Z. Phys. Chem.* **2005**, *219*, 125.
(5) Courty, A.; Mons, M.; Le Calvé, J.; Piuzzi, F.; Dimicoli, I. *J. Phys. Chem. A* **1997**, *101*, 1445.
(6) Courty, A.; Mons, M.; Dimicoli, I.; Piuzzi, F.; Gaigeot, M.-P.; Brenner, V.; du Pujo, P.; Millié, P. *J. Phys. Chem. A* **1998**, *102*, 6590.
(7) Ibrahim, Y.; Alsharaeh, E.; Dias, K.; Meot-Ner (Mautner), M.; El-Shall, M. S. *J. Am. Chem. Soc.* **2004**, *126*, 12766.
(8) Ibrahim, Y. M.; Meot-Ner (Mautner), M.; Alsharaeh, E. H.; El-Shall, M. S.; Scheiner, S. *J. Am. Chem. Soc.* **2005**, *127*, 7053.
(9) Tachikawa, H.; Igarashi, M. J. *Phys. Chem. A* **1998**, *102*, 8648.
(10) Tachikawa, H.; Igarashi, M.; Ishibashi, T. *Phys. Chem. Chem. Phys.* **2001**, *3*, 3052.
(11) Miyazaki, M.; Fujii, A.; Ebata, T.; Mikami, N. *Chem. Phys. Lett.* **2001**, *349*, 431.
(12) Miyazaki, M.; Fujii, A.; Ebata, T.; Mikami, N. *Phys. Chem. Chem. Phys.* **2003**, *5*, 1137.
(13) Miyazaki, M.; Fujii, A.; Ebata, T.; Mikami, N. *J. Phys. Chem. A* **2004**, *108*, 8269.
(14) Miyazaki, M.; Fujii, A.; Ebata, T.; Mikami, N. *J. Phys. Chem. A* **2004**, *108*, 10656.
(15) Miyazaki, M.; Fujii, A.; Ebata, T.; Mikami, N. *Chem. Phys. Lett.* **2004**, *399*, 412.
(16) Solcá, N.; Dopfer, O. *Chem. Phys. Lett.* **2001**, *347*, 59.
(17) Solcá, N.; Dopfer, O. *J. Phys. Chem. A* **2003**, *107*, 4046.
(18) Pribble, R. N.; Zwier, T. S. *Science* **1994**, *265*, 75.
(19) Pribble, R. N.; Zwier, T. S. *Faraday Discuss.* **1994**, *97*, 229.
(20) Gotch, A. J.; Zwier, T. S. *J. Chem. Phys.* **1990**, *93*, 6977.
(21) Hunter, E. P. L.; Lias, S. G. *J. Phys. Chem. Ref. Data* **1998**, *27*, 413.
(22) *CRC Handbook of Chemistry and Physics*, 76th edition; Lide, D. R., Ed.; CRC Press: Boca Raton, FL, 1995.
(23) Sampson, R. K.; Lawrance, W. D. *Aust. J. Chem.* **2003**, *56*, 275.
(24) Solcá, N.; Dopfer, O. *Chem. Phys. Lett.* **2003**, *369*, 68.
(25) Garrett, A. W.; Zwier, T. S. *J. Chem. Phys.* **1992**, *96*, 7259.
(26) Walter, K.; Weinkauf, R.; Bosel, U.; Schlag, E. W. *Chem. Phys. Lett.* **1989**, *155*, 8.
(27) Goode, J. G.; Hofstein, J. D.; Johnson, P. M. *J. Chem. Phys.* **1997**, *107*, 1703.
(28) Pribble, R. N.; Hagemeister, F. C.; Zwier, T. S. *J. Chem. Phys.* **1997**, *106*, 2145.
(29) Frisch, M. J.; Trucks, G. W.; Schlegel, H. B.; Scuseria, G. E.; Robb, J. M. A.; Cheeseman, R.; Zakrzewski, V. G.; Montgomery Jr., J. A.; Stratmann, R. E.; Burant, J. C.; Dapprich, S.; Millam, J. M.; Daniels, A. D.; Kudin, K. N.; Strain, M. C.; Farkas, O.; Tomasi, J.; Barone, V.; Cossi, M.; Cammi, R.; Mennucci, B.; Pomelli, C.; Adamo, C.; Clifford, S.; Ochterski, J.; Petersson, G. A.; Ayala, P. Y.; Cui, Q.; Morokuma, K.; Malick, D. K.; Rabuck, A. D.; Raghavachari, K.; Foresman, J. B.; Cioslowski, J.; Ortiz, J. V.; Baboul, A. G.; Stefanov, B. B.; Liu, G.; Liashenko, A.; Piskorz, P.; Komaromi, I.; Gomperts, R.; Martin, R. L.; Fox, D. J.; Keith, T.; Al-Laham, M. A.; Peng, C. Y.; Nanayakkara, A.; Gonzalez, C.; Challacombe, M.; Gill, P. M. W.; Johnson, B.; Chen, W.; Wong, M. W.; Andres, J. L.; Gonzalez, C.; Head-Gordon, M.; Replogle, E. S.; Pople, J. A. *Gaussian 98*, revision A.7; Gaussian, Inc.: Pittsburgh, PA, 1998.
(30) Shimanouchi, T. *Tables of Molecular Vibrational Frequencies, Consolidated Volume I*; National Standard Reference Data Series; National Bureau of Standards: Washington, DC, 1972; Vol. 39.
(31) Dopfer, O.; Olkhov, R. V.; Maier, J. P. *J. Chem. Phys.* **1999**, *111*, 10754.
(32) Fujii, A.; Fujimaki, E.; Ebata, T.; Mikami, N. *J. Chem. Phys.* **2000**, *112*, 6275.
(33) Fujimaki, E.; Fujii, A.; Ebata, T.; Mikami, N. *J. Phys. Chem. A* **2001**, *105*, 4882.
(34) Fujii, A.; Iwasaki, A.; Ebata, T.; Mikami, N. *J. Phys. Chem. A* **1997**, *101*, 5963.
(35) Mons, M.; Dimicoli, I.; Tardivel, B.; Piuzzi, F.; Brenner, V.; Millié, P. *Phys. Chem. Chem. Phys.* **2002**, *4*, 571.
(36) Tachikawa, H. *Phys. Chem. Chem. Phys*. **2002**, *4*, 6018.
(37) Chang, H.-C.; Jiang, J.-C.; Lin, S. H.; Lee, Y. T.; Chang, H.-C. *J. Phys. Chem. A* **1999**, *103*, 2941.
(38) Fujii, A.; Enomoto, S.; Miyazaki, M.; Mikami, N. *J. Phys. Chem. A* **2005**, *109*, 138.
(39) Tonokura, K.; Norikane, Y.; Koshi, M.; Nakano, Y.; Nakamichi, S.; Goto, M.; Hashimoto, S.; Kawasaki, M.; Andersen, M. P. S.; Hurley, M. D.; Wallington, T. J. *J. Phys. Chem. A* **2002**, *106*, 5908.
(40) Davico, G. E.; Bierbaum, V. M.; DePuy, C. H.; Ellison, G. B.; Squires, R. R. *J. Am. Chem. Soc*. **1995**, *117*, 2590.